Eur. Phys. J. A **31**, 662–664 (2007)
DOI 10.1140/epja/i2006-10192-7

THE EUROPEAN PHYSICAL JOURNAL A

Special Article – QNP 2006

Composite-meson model and meson exchange currents

R.Ya. Kezerashvili[a] and V.S. Boyko

Physics Department, New York City College of Technology, The City University of New York, Brooklyn, NY 11201, USA

Received: 8 October 2006
Published online: 22 February 2007 –

Abstract. We study the meson exchange currents (MEC) mechanism for the pion double-charge exchange (DCX) reaction in a composite-meson model. The model assumes that the mesons are two-quark systems and can interact with each other only through quark loops. The contributions of the ρ, σ, and f_0 mesons, the four-quark box diagram as well as a contact diagram has been taken into account. It is shown that the contribution of the ρ, σ, and f_0 mesons increases the forward scattering cross-section in an average by 25% and decreases with energy.

PACS. 25.80.Gn Pion charge-exchange reactions – 25.80.Hp Pion-induced reactions

The most important problem of the DCX of π-mesons on nuclei is the mechanism of the reaction. Normally, the reaction is dominated by the sequential mechanism (SQM), in which the incoming pion undergoes two sequential single-charge exchange scatterings on nucleons within a nucleus. In ref. [1] the MEC mechanism, was proposed and it consists of the assumption that the incident pion is scattered on the off-shell virtual pion exchanged by the nucleons within the nucleus and the DCX takes place at the $\pi\pi$ vertex as shown in fig. 1a. Later, ref. [2] introduced an additional diagram shown in fig. 1b and concluded that the MEC effects would be small for an analog DCX because this diagram partially cancels the contribution of the pole term. The MEC issue has been revived in refs. [3] and [4] using the Lovelace-Veneziano model and in refs. [5–9] based on an effective Lagrangian method. All calculations of the MEC in the effective Lagrangian formalism are performed in the lowest order which includes the contribution of the "trees" diagram and no pionic or baryonic closed loop diagrams are included. The tree diagrams correspond to the Born approximation for $\pi\pi$ scattering, and their contribution is defined by the first term of the expansion of the $\pi\pi$ amplitude in terms of $1/F_\pi^2$. In ref. [9], the authors showed that because of the small DCX cross-section produced by the SQM at high energies, the MEC mechanism could show up, even in the Born approximation. Below we study the MEC mechanism for the DCX reaction based on the composite-meson model. The model assumes that the mesons are two-quark systems and can interact with each other only through quark loops. We are considering the diagrams shown in fig. 2 which successfully describe $\pi\pi$ scattering, as well as the contact diagram in fig. 1b. This approach allows to find the contribution of the σ, f_0 and ρ mesons to the MEC mechanism.

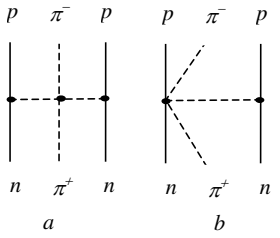

Fig. 1. The pole (a) and contact (b) diagrams.

The chiral symmetry requires consideration of both diagrams in fig. 1, which describe the pion DCX on two nucleons through the MEC mechanism. We replaced the diagram 1a by the diagram on the left side in fig. 2, where the shaded vertex block corresponds to the $\pi\pi$ interaction and constructed the amplitude for the process $\pi^+nn \to \pi^-pp$ using the amplitudes for $\pi\pi$ scattering and for the πN-$\pi\pi N$ process. The amplitude corresponding to the graph on the left side in fig. 2 in the nonrelativistic limit is

$$T_1 = (i\sqrt{2}g)^2 \frac{(\boldsymbol{\sigma}_1 \cdot \mathbf{q}_1)(\boldsymbol{\sigma}_2 \cdot \mathbf{q}_2)}{4m^2} \frac{M_{\pi^+\pi^-}(q_{1\mu}; q_{2\mu})}{(\mathbf{q}_1^2 + m_\pi^2)(\mathbf{q}_2^2 + m_\pi^2)}, \quad (1)$$

where g is the πN coupling constant, m is the mass of the nucleon, $\mathbf{q}_1 = \mathbf{p}_1' - \mathbf{p}_1$ and $\mathbf{q}_2 = \mathbf{p}_2' - \mathbf{p}_2$, m_π is the pion mass, and $q_{1\mu}$ and $q_{2\mu}$ are the 4-momenta of virtual mesons. In eq. (1) $M_{\pi^+\pi^-}$ is the transition matrix element for the $\pi^+\pi^- \to \pi^+\pi^-$ process. Similarly, we can find the amplitude for fig. 1b using the transition matrix for the πN-$\pi\pi N$ process.

[a] e-mail: rkezerashvili@citytech.cuny.edu

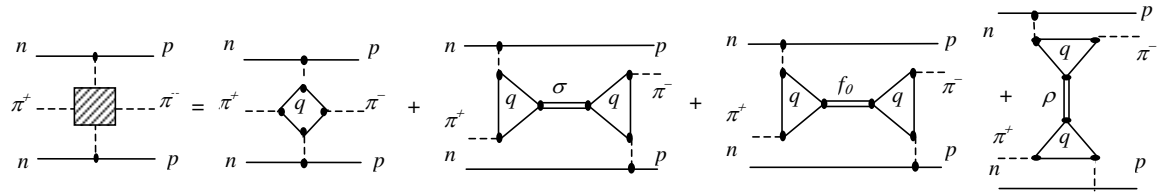

Fig. 2. The quark structure of the MEC diagram.

In the composite-meson model the shaded vertex box in fig. 2 can be considered at the quark level and includes the sum of the quark diagrams which successfully describe $\pi\pi$ scattering. Indeed, $\pi^+ = u\overline{d}$ and $\pi^- = d\overline{u}$ are two-quark systems, and can interact with each other only through quark loops. Therefore, in the single-loop approximation, the diagram on the left side in fig. 2 can be expanded as shown. The first quark box diagram actually corresponds to the pole diagram in fig. 1a for $\pi\pi$ scattering and a part of its contribution which is proportional to $1/F_\pi^2$ represents the Born approximation in the effective Lagrangian method. The choice of the other diagrams representing ρ, σ and f_0 mesons is based on the probability of the two-pion decay of mesons: $\rho(770) \to \pi\pi$, $\sigma(600) \to \pi\pi$ and $f_0(980) \to \pi\pi$. The inner quark blocks of the diagrams in fig. 2 can be easily obtained from the Lagrangian [10] and the set of the Lagrangians relevant to the processes of figs. 1b and 2 are

$$L = \overline{Q}\left[i\partial - m_q + \frac{m_q}{F_\pi}(\sigma \sin\alpha + f_0 \cos\alpha + i\gamma_5 \boldsymbol{\tau}\boldsymbol{\pi}) + \frac{g_\rho}{2}\boldsymbol{\tau}\boldsymbol{\rho}\right]Q, \tag{2}$$

$$L_{NN\pi} = \frac{g}{2m}\overline{\psi}\gamma^\mu\gamma_5\boldsymbol{\tau}\psi\cdot(\partial_\mu\boldsymbol{\pi}), \tag{3}$$

$$L_{NN\pi\pi\pi} = -\frac{g}{2m}\frac{1}{4F_\pi^2}\overline{\psi}\gamma^\mu\gamma_5\boldsymbol{\tau}\psi\cdot(\partial_\mu\boldsymbol{\pi})\boldsymbol{\pi}^2, \tag{4}$$

where Q is the quark field, m_q is the mass of the quark, g_ρ is the decay constant of the ρ-meson, and α is the mixing angle. To find the contributions of the diagrams in fig. 2 we need to know all effective coupling constants and express them in terms of two decay constants g_ρ and F_π of the $\rho \to 2\pi$ and $\pi \to \mu\overline{\nu}$ decays. We shall impose a natural requirement that on the mass shell the form factors of the processes should coincide exactly with the corresponding physical coupling constants. The form factors for the $\rho \to 2\pi$, $\sigma \to 2\pi$ and $f_0 \to 2\pi$ decays can be obtained from the Lagrangian (2) and finally the results for the inner blocks of the diagrams in fig. 2 (for $\pi^+\pi^- \to \pi^+\pi^-$ amplitude) and the diagram in fig. 1b are

$$\begin{aligned} M_{\pi^+\pi^-} &= -\frac{m_\pi^2}{F_\pi^2} + \frac{m_q^2}{(\pi F_\pi)^2}\left[\frac{s+t}{F_\pi^2} - \frac{m_q^2}{(4\pi F_\pi)^2}\frac{s+t}{F_\pi^2}\right] \\ &+ \frac{4m_q^2}{F_\pi^2}\left\{\frac{4m_q^2}{m_\sigma^2}\left(\frac{s}{(m_\sigma^2-s)} + \frac{t}{(m_\sigma^2-t)}\right)\sin^2\alpha\right. \\ &\left. + \frac{4m_q^2}{m_{f_0}^2}\left(\frac{s}{(m_{f_0}^2-s)} + \frac{t}{(m_{f_0}^2-t)}\right)\cos^2\alpha\right\} \\ &+ g_\rho\left\{\frac{t-u}{m_\rho^2-s}\left(1+\frac{s-m_\rho^2}{8\pi^2F_\pi^2}\right)^2 + \frac{s-u}{m_\rho^2-t}\left(1+\frac{t-m_\rho^2}{8\pi^2F_\pi^2}\right)^2\right\}, \end{aligned} \tag{5}$$

$$T_2 = -\frac{g^2}{4m^2}\frac{2}{F_\pi^2}\frac{(\boldsymbol{\sigma}_1\cdot\mathbf{q}_1)\,[\boldsymbol{\sigma}_2\cdot\mathbf{q}_1 - \boldsymbol{\sigma}_2\cdot\mathbf{q}_2]}{(\mathbf{q}_1^2+m_\pi^2)}. \tag{6}$$

In eq. (5) s, t, and u are the standard Mandelstam variables, the mixing angle α is determined from $\Gamma_{f_0\to 2\pi} = 26\,\mathrm{MeV}$ and it is $\alpha = 17^\circ$ if $m_q = 280\,\mathrm{MeV}$ [11], and the decay constant of the ρ-meson g_ρ is $g_\rho^2/4\pi \approx 3$. The contribution of the quark box diagram depends on the undetermined parameter, whose value was fixed so that the experimental value of the pion-pion scattering length a_0^2 is obtained.

Let us compare the MEC amplitude in the composite-meson model given by (5) with one in the Born approximation for the Weinberg Lagrangian [12]: $M_{\pi^+\pi^-} = -m_\pi^2/F_\pi^2 + (s+t)/F_\pi^2$. It is easy to see that the constant term in eq. (5) is the same. The term in the square brackets is caused by the quark box diagram and inclusion of the so-called q^2 terms (the q^2 terms leads to convergent integrals [13]) in the quark box diagrams, and it is partially proportional to $(1/F_\pi^2)^2$. The factor in front of the square brackets $m_q^2/(\pi F_\pi)^2 = 1$ for $F_\pi = 89.2\,\mathrm{MeV}$ and $m_q = 280$ MeV and a variation of this factor is nonsignificant when the pion decay constant varies from 87 MeV to 93 MeV. Therefore, the constant term and the first term in the square brackets in eq. (5) give the Weinberg transition amplitude for the $\pi^+\pi^- \to \pi^+\pi^-$ process. The two terms in (5) related to the mixing angle α are representing the contribution of the σ and f_0 mesons. The term that follows the factor g_ρ is the contribution of the ϱ-meson and it has the parts which are also proportional to $(1/F_\pi^2)^2$. After the substitution of eq. (5) into (1) one can separate the part which corresponds to the amplitude of the pole diagram in fig. 1a for the Weinberg Lagrangian. The sum of this part and (6) gives the contribution of the quark box diagram, including only terms proportional to $1/F_\pi^2$ and the contact diagram and is the same as the sum of contributions of the pole (fig. 1a) and contact (fig. 1b) diagrams in the Born approximation. The rest of the contribution of the quark box diagram is proportional to $(1/F_\pi^2)^2$ and represents the deviation from the Born approximation.

We calculated the forward scattering cross-section for the $^{18}\mathrm{O}(\pi^+,\pi^-)^{18}\mathrm{Ne}$ reaction for the incident pion energy from 600 MeV to 1400 MeV and compare the contribution of the MEC evaluated in the composite-meson model with the calculations in the Born approximation. We use the shell model wave functions to describe ^{18}O and ^{18}Ne nuclei, and assuming that the DCX process takes place on the valence neutrons and leads to the double isobaric analog state. The wave function of the two odd neutrons in ^{18}O has been used as in [3,6] with the harmonic-oscillator parameter $\alpha^2 = 0.32\,\mathrm{fm}^{-2}$. Since our main points are to

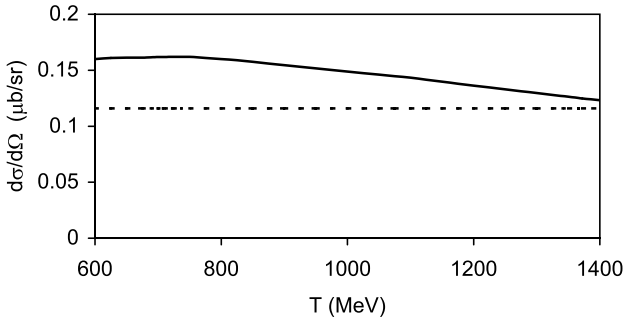

Fig. 3. Forward scattering cross-section for the reaction $^{18}O(\pi^+,\pi^-)^{18}Ne$ as a function of the incident pion energy. The contributions of the MEC in the composite-meson model with the contact diagram are shown by the solid curve, and the pole and contact diagrams in the Born approximation by the dashed line.

understand the contribution of three $\pi\pi$ resonances ρ, σ and f_0 to the MEC mechanism, establish the order of magnitude of this contribution and compare it to the conventional MEC mechanism, follow [7], for simplicity, we neglect the distortion of the pion waves, using the plane waves instead. In the plane-wave approximation integration of the sum of the contributions of the quark box diagram, including only terms proportional to $1/F_\pi^2$ and the contact diagram in fig. 1b over momentum q in the target, can be performed analytically and the result is

$$T^B = \frac{2}{F_\pi^2}\frac{1}{m_\pi}\frac{\partial}{\partial m_\pi}V(r), \qquad (7)$$

where $V(r)$ is a one-pion exchange potential.

The results of the calculations for the forward scattering cross-section as a function of the incoming pion kinetic energy are presented in fig. 3. The results of calculations for the composite-meson model with the contact diagram in fig. 3 are presented by a solid line. The cross-section for the MEC mechanism in the Born approximation, when both the pole term as well as the contact term are considered, is presented by the dashed line. The comparison of these results shows that the inclusion of the ρ, σ and f_0 mesons increases the cross-section and their contribution decreases with energy. The cross-section for the MEC in the composite-meson model with the contact diagram in fig. 1b is systematically larger in an average by 25% than that in the Born approximation. We checked the sensibility of the calculations to the changes of the masses of the σ and f_0 mesons. The cross-section is sensitive to the small changes of the σ-meson mass and almost did not change with small changes of the f_0-meson mass. For example, the change of the σ-meson mass from 780 MeV to 700 MeV will increase the cross-section by about 14%. Let us also mention that the third term in eq. (5) related to the ϱ-meson contribution, appreciably changes the cross-section, and it shows the importance of the ϱ-meson at energies above 600 MeV. At energies above 1000 MeV the cross-section for the MEC mechanism with inclusion of the ρ, σ and f_0 mesons becomes larger than one for the SQM and that mechanism dominates in the reaction.

Thus, we can conclude that at the considered energy region the MEC mechanism in the composite-meson model with the contact diagram can reveal in the pion DCX, because it has a substantial contribution and the inclusion of the ρ, σ and f_0 mesons increases the contribution of the meson exchange currents in the MEC mechanism for the DCX reaction. It is important to mention that the distortion of the pion waves will generally reduce the cross-section in the composite-meson model as well as for the MEC in the Born approximation and for the SQM, but it will not change the conclusion of the importance of including the pion resonances into the MEC mechanism.

References

1. J.F. Germond, C. Wilkin, Lett. Nuovo Cimento **13**, 605 (1975).
2. M.R. Robilotta, C. Wilkin, J. Phys. G: Nucl. Phys. **4**, L115 (1978).
3. E. Oset, D. Strottman, M.J. Vicente Vacas, Ma Wei-hsing, Nucl. Phys. A **408**, 461 (1983).
4. N. Auerbach, W.R. Gibbs, J.N. Ginocchio, W.B. Kaufmann, Phys. Rev. C **38**, 1277 (1988).
5. R.I. Jibuti, R.Ya. Kezerashvili, Nucl. Phys. A **437**, 687 (1985).
6. Yu. Zi-quang, Cai Chong-hai, Ma Wei-hsing, Zhao Shuping, Phys. Rev. C **38**, 272 (1988).
7. M.F. Jiang, D.S. Koltun, Phys. Rev. C **42**, 2662 (1990); D.S. Koltun, M.F. Jiang, Phys. Lett. B **273**, 6 (1991).
8. M.B. Johnson, E. Oset, H. Sarafian, E.R. Siciliano, M.J. Vicente Vacas, Phys. Rev. C **44**, 2480 (1991).
9. L. Alvarez-Ruso, M.J. Vicente Vacas, J. Phys. G: Nucl. Part. Phys. **22**, L45 (1996).
10. M.K. Volkov, A.A. Osipov, Sov. J. Nucl. Phys. **39**, 440 (1984).
11. K. Kikkawa, Prog. Theor. Phys. **56**, 947 (1976)
12. S. Weinberg, Phys. Rev. Lett. **17**, 616 (1966); **18**, 188 (1967).
13. M.K. Volkov, D.V. Kreopalov, Theor. Math. Phys. **57**, 21 (1983).